

UC Irvine

Faculty Publications

Title

How Rossby wave breaking over the Pacific forces the North Atlantic Oscillation

Permalink

<https://escholarship.org/uc/item/6vk47077>

Journal

Geophysical Research Letters, 35(10)

ISSN

0094-8276

Authors

Strong, Courtenay
Magnusdottir, Gudrun

Publication Date

2008-05-29

DOI

10.1029/2008GL033578

Supplemental Material

<https://escholarship.org/uc/item/6vk47077#supplemental>

Copyright Information

This work is made available under the terms of a Creative Commons Attribution License, available at <https://creativecommons.org/licenses/by/4.0/>

Peer reviewed

How Rossby wave breaking over the Pacific forces the North Atlantic Oscillation

Courtenay Strong¹ and Gudrun Magnusdottir¹

Received 7 February 2008; revised 3 April 2008; accepted 9 April 2008; published 29 May 2008.

[1] Anticyclonic Rossby wave breaking (RWB) over a well-defined, limited-area region of the east Pacific leads to the positive polarity of the North Atlantic Oscillation (NAO) by locally piling up wave activity where it may be advected downstream, resulting in increased wave activity flux and anticyclonic RWB over the subtropical Atlantic. A composite time series shows that Pacific RWB occurs several days prior to the Atlantic RWB and the peak of the NAO index. Following Pacific RWB, a channel of increased pseudomomentum flux extends from the Pacific wave breaking region, northeastward toward midlatitudes of eastern North America where pseudomomentum density accumulates for several days prior to moving eastward and leading to anticyclonic RWB over the Atlantic. **Citation:** Strong, C., and G. Magnusdottir (2008), How Rossby wave breaking over the Pacific forces the North Atlantic Oscillation, *Geophys. Res. Lett.*, 35, L10706, doi:10.1029/2008GL033578.

1. Introduction

[2] Several studies have examined how the winter North Atlantic Oscillation (NAO) is related to tropospheric Rossby wave breaking (RWB), where RWB is the rapid, irreversible overturning of potential vorticity (PV) contours on an isentropic surface [McIntyre and Palmer, 1983]. Riviere and Orlanski [2007] linked the positive (negative) polarity of the winter NAO to the momentum flux signature of North Atlantic anticyclonic (cyclonic) RWB. Strong and Magnusdottir [2008] (hereinafter referred to as SM08) showed how wave breaking projects onto the NAO and provides upper tropospheric forcing of the NAO's zonal wind pattern. Considering Atlantic RWB, SM08 showed that the positive polarity of the NAO results from cyclonic RWB near 70°N and anticyclonic RWB within their "A3 region" near 50°N, whereas the negative polarity results from cyclonic RWB near 50°N and anticyclonic RWB near 30° and near 70°N.

[3] Several researchers have suggested that the winter NAO may respond to tropospheric internal forcing from outside the Atlantic basin [Benedict *et al.*, 2004, and references therein] (hereinafter referred to as BLF). The observational study of BLF describes the positive NAO as the remnant of two consecutive anticyclonic RWB events, one near the west coast of North America and the other over the subtropical North Atlantic. BLF suggest that a trough

associated with Pacific RWB advects across North America to provide the northern pole of the NAO anomaly pattern, while the Atlantic RWB event provides the NAO's southern pole. BLF did not explore how the Pacific and Atlantic RWB events may be dynamically related.

[4] The present research shows that east-Pacific anticyclonic RWB not only precedes, but directly leads to the Atlantic anticyclonic RWB, resulting in the positive polarity of the NAO. Our approach uses two diagnostic tools not previously paired in a study of the NAO: 1) a direct measure of the presence and spatial scale of RWB based on the geometry of PV contours, and 2) a pseudomomentum density and flux for which there is a finite-amplitude conservation relation.

2. Data and Methods

[5] From NCEP/NCAR reanalysis data for winters (DJF) 1958–2006, we use six-hourly pressure p , temperature T , Montgomery streamfunction M , and the horizontal velocity (u , v) on 11 isentropic surfaces from 270K to 650K. We calculate a 6-hourly NAO index (NAOI) by projecting sea-level pressure onto the leading empirical orthogonal function of seasonal-mean sea-level pressure for the 49 winters over the Atlantic domain (90°W–40°E, 20–80°N). We low-pass filter the NAOI using a Butterworth filter that has zero phase distortion and retains most of the energy associated with periods of ten days or longer (denoted NAOI_f). We define two types of transition events for the NAOI_f: an upward transition means the NAOI_f increased from a negative local minimum to a positive local maximum, and a downward transition means the NAOI_f decreased from a positive local maximum to a negative local minimum. To be a transition event, the local maxima and minima must meet the requirement $|NAOI_{f}| \geq 0.4$, which assures that the selected sign reversals are nontrivial without unnecessarily restricting the number of events selected. These transition event definitions yield 52 upward transitions and 51 downward transitions for the 1958–2006 winter record, which averages to slightly more than one of each type per winter. An example of an upward transition is shown in Figure 1b.

[6] We use the database of anticyclonic RWB on the 350-K surface described in detail by SM08. Overturning of PV contours on the 350-K isentropic surface was found to be representative of upper tropospheric breaking (SM08). Briefly, we identify anticyclonically overturning PV contours such as the example in Figure 1a. We record the area of the break's poleward tongue (shading, Figure 1a) and the longitude-latitude coordinates of the tongue's centroid (solid circle, Figure 1a). Then, for $N = 400$ equal-area bins

¹Department of Earth System Science, University of California, Irvine, California, USA.

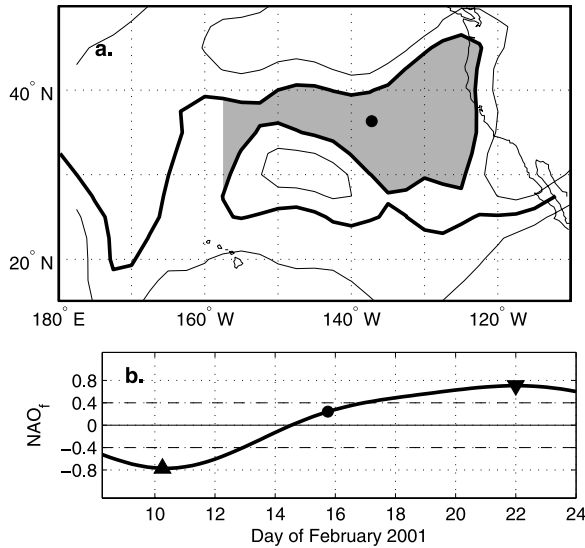


Figure 1. (a) Anticyclonic Rossby wave breaking at 1200 UTC on 08 February 2001. The 350-K potential vorticity is contoured every 2 pvu with the 4-pvu contour bold. Shading shows the area of the break's poleward-advecting tongue, and the circle marks the tongue's centroid. (b) An upward transition of the NAO with the time of the anticyclonic break in Figure 1a marked by a solid circle and the NAO local minimum (maximum) marked by an upward-facing (a downward-facing) triangle.

centered at $(\lambda, \phi)_n$, $n = 1, \dots, N$, we calculate the relative frequency of anticyclonic RWB centroids

$$\gamma_a(\lambda, \phi)_n \equiv \frac{1}{\tau} \sum_{t=1}^{\tau} \beta[(\lambda, \phi)_n, t] \quad (1)$$

where λ is longitude, ϕ is latitude, τ is the number of 6-hourly observations in the period for which γ is calculated, and the event parameter, β , takes the value 1 when a centroid is located in the bin at time t and zero otherwise. The values for γ_a may also be thought of as the empirical probability of observing a centroid associated with anticyclonic RWB within a bin ($0 \leq \gamma_a \leq 1$).

[7] To determine how γ_a varies during upward and downward transitions of the NAO, we temporarily restrict our analysis to the set m of all six-hourly observations whose $|\text{NAOI}_f|$ values fall below the limit that is used to define transitions ($|\text{NAOI}_f| \leq 0.4$). The letter m is chosen to reflect moderate values of the NAO. We restrict this portion of the analysis to m because there are strong γ_a signals associated with high and low values of the NAOI_f (SM08), and we want to focus attention here on how γ_a varies during the NAO transitions rather than during NAO local extrema. From this set m , we calculate the reference relative frequency $\gamma_a(m)$. We then find the subsets m_{\uparrow} and m_{\downarrow} which are all six-hourly observations in the set m that fall, respectively, within upward and downward transitions of the NAO. We then calculate the anomalies

$$\gamma'_{a\uparrow} \equiv \gamma_a(m_{\uparrow}) - \gamma_a(m) \quad (2)$$

$$\gamma'_{a\downarrow} \equiv \gamma_a(m_{\downarrow}) - \gamma_a(m). \quad (3)$$

The statistical significance of the γ anomalies is tested by calculating 95% confidence limits based on continuity-corrected [Fleiss, 1981] Wilson score intervals [Newcombe, 1998].

[8] We diagnose wave behavior related to RWB and the NAO using the three-dimensional Haynes angular pseudomomentum flux \mathbf{F} , which, has a conservation relation of the form [Haynes, 1988]

$$\frac{\partial A}{\partial t} + \nabla \cdot \mathbf{F} = S \quad (4)$$

valid for finite-amplitude disturbances to the primitive equations. Here, S stands for non-conservative source/sink terms and A is the pseudomomentum density. Both A and \mathbf{F} are second-order in wave amplitude and are written out by Magnusdottir and Haynes [1999]. This relation is valid for a broad class of transient and finite-amplitude disturbances including the breaking Rossby waves considered in the present study. We calculate A and the horizontal components of \mathbf{F} on the 350-K isentropic surface, defining the basic state as the time and longitudinal average of the 350-K winter flow field (DJF 1958–2006). We remove phase-dependence from the flux by adding a non-divergent correction term as detailed in Magnusdottir and Haynes [1999].

3. Results

[9] Upward transitions of the NAOI_f are associated with significantly increased relative frequency of anticyclonic RWB over the east Pacific with a maximal signal near 132°W 32°N ($\gamma'_{a\uparrow}$, Figure 2a), and local γ_a values as high as 1.75 times their $\gamma_a(m)$ reference values. Most (87%) of the upward transitions of the NAOI_f had at least one anticyclonic centroid in the east-Pacific box. More than a quarter of the upward transitions had an anticyclonic centroid present at each of the six-hourly observations in the upward transition period. Slightly more than a quarter of all downward transitions had no anticyclonic centroids in the east-Pacific box, and downward transition periods are associated with significantly decreased relative frequency of anticyclonic breaking ($\gamma'_{a\downarrow}$, Figure 2b). Local values of $\gamma'_{a\downarrow}$ are as small as 0.39 times their $\gamma_a(m)$ reference values. The γ_a anomalies outside the Pacific region for m_{\uparrow} and m_{\downarrow} are not significant or are weaker in magnitude than those over the Pacific (not shown). The lack of an Atlantic counterpart to the Pacific γ'_a results described above is noteworthy since the circulation changes associated with NAO transitions are better-defined over the Atlantic than the Pacific.

[10] To determine the temporal behavior of the relationship between Pacific RWB and transitions of the NAOI_f , we show in Figure 3 the composite frequency of anticyclonic RWB in the east-Pacific box, denoted $\gamma_a(\text{EPac})$, on a composite time line of upward (Figure 3a) and downward transitions (Figure 3b) of the NAOI_f . The phase of the curves shows that Pacific RWB leads the NAOI_f in both cases. The average time between the local extrema of the NAOI_f (shown by triangles in Figure 3a) is approximately

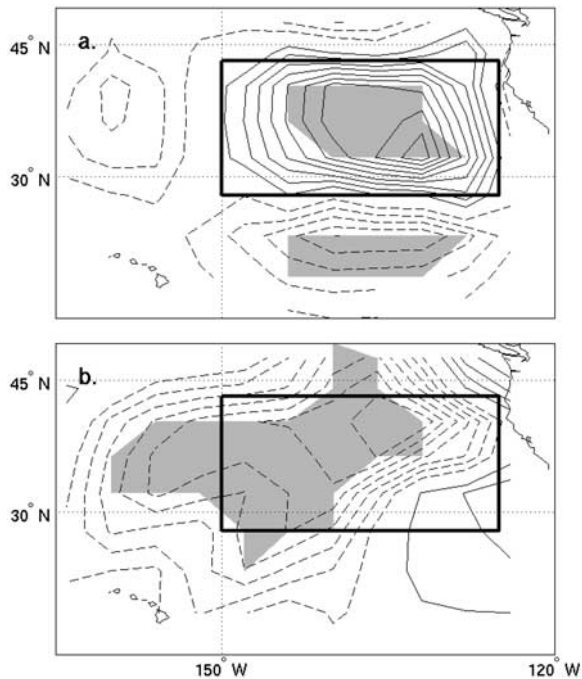


Figure 2. Anomalies of anticyclonic Rossby wave breaking relative frequency associated with (a) upward transitions ($\gamma_{a\uparrow}$) and (b) downward transitions ($\gamma_{a\downarrow}$) of the NAOI_f. Contour interval is 5×10^{-3} with negative values dashed, shading indicates significance at the 95% confidence level, and the east-Pacific box is bound by bold lines in each panel.

10 days, meaning that $\gamma_a(\text{EPac})$ exceeds its composite average approximately seven days before the peak of the upward-transitioning NAOI_f (Figure 3a).

[11] The approximately 7-day lag between above-average $\gamma_a(\text{EPac})$ and the peak of the NAOI_f (Figure 3a) provides ample time for the pseudomomentum associated with Pacific RWB to advect across North America and lead to the Atlantic anticyclonic RWB associated with the positive polarity of the NAO. To visualize this process, we developed an animation showing the composite evolution of A and the horizontal components of \mathbf{F} on the 350-K isentropic surface for all east-Pacific RWB observations during upward transitions (the “break-transition-up” composite). Selected frames corresponding to days 1, 4, and 8 of the break-transition-up composite are in Figures 4a, 4b, and 4c, respectively (see Animation S1).¹ The first frame of the animation (day 0) is the mean of the 235 observations for which an anticyclonic centroid was present in the east-Pacific box and the NAOI_f was moderate ($|\text{NAOI}_f| < 0.4$) and transitioning up. The composite average over the 235 cases is denoted by an overbar, and subscripts are used to denote composite averages from day zero to day nine (e.g., $\bar{A}_0, \bar{A}_{0.25}, \dots, \bar{A}_9$). Two moderate NAOI_f “null” composite views were also developed (not shown) and will be contrasted with the findings in Figure 4. They are: 1) moderate NAOI_f without an anticyclonic centroid in the east-Pacific box (the “no-break composite” with 3668 cases), and 2) moderate NAOI_f with an anticyclonic cen-

triod in the east-Pacific box but without an upward transition of the NAOI_f (the “break-no-transition-up composite” with 1684 cases). To equalize sample sizes for the purpose of comparing the break-transition-up, no-break, and break-no-transition-up composites, 235-member random samples were taken from each of the null composites and the results were found to be robust across an ensemble of such samples.

[12] In the break-transition-up composite, the pseudomomentum flux tends to trace the shape of the overturning potential vorticity contours during anticyclonic breaking, as shown in *Magnusdottir and Haynes* [1999]. This is evident in the horizontal $\bar{\mathbf{F}}_1$ field (Figure 4a), which traces the eastern edge of the anticyclonically-breaking wave’s poleward-advecting tongue within the east-Pacific box (compare to Figure 1a). The region equatorward of the east-Pacific box indicates convergence of horizontal pseudomomentum flux, and the high \bar{A}_1 values near 135°W 10°N are increased markedly from the corresponding values of \bar{A}_0 . The no-break composite, by contrast, lacks clear convergence of the horizontal flux and buildup of \bar{A} equatorward of the east-Pacific box. The pseudomomentum accumulated by the east-Pacific anticyclonic RWB is advected northeastward across Mexico toward the eastern United States where another region of convergent pseudomomentum flux leads to increased concentration of \bar{A} over the next several days (compare the shading along the east coast of the United States in Figures 4a and 4b). Decom-

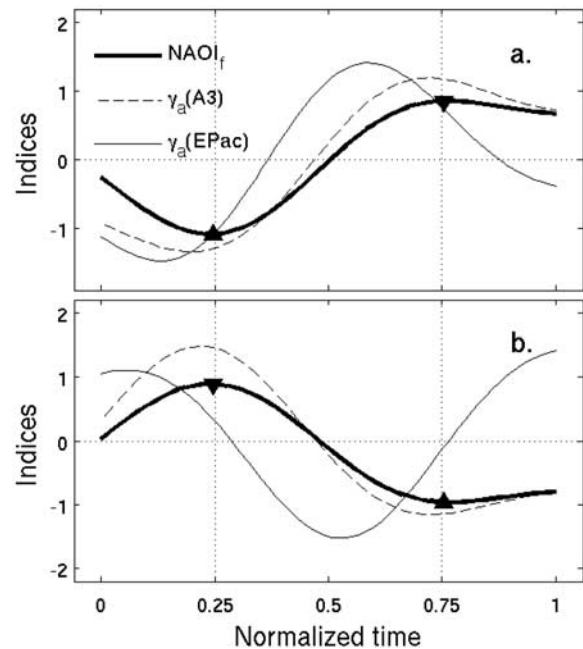


Figure 3. Composite time series of NAO (a) upward transitions and (b) downward transitions. NAOI_f is the low-pass filtered NAO index. $\gamma_a(\text{EPac})$ is the composite frequency of anticyclonic breaking in the east-Pacific box defined in Figure 2a. $\gamma_a(\text{A3})$ is the composite frequency of anticyclonic breaking in the A3 region shown in Figure 4c. Data for each transition event were interpolated linearly onto a time axis normalized to run from zero to one with the local minima or maxima at 0.25 and 0.75, and the resultant time series were standardized and smoothed with the zero phase distortion, low-pass filter used to develop the NAOI_f.

¹Auxiliary materials are available in the HTML. doi:10.1029/2008GL033578.

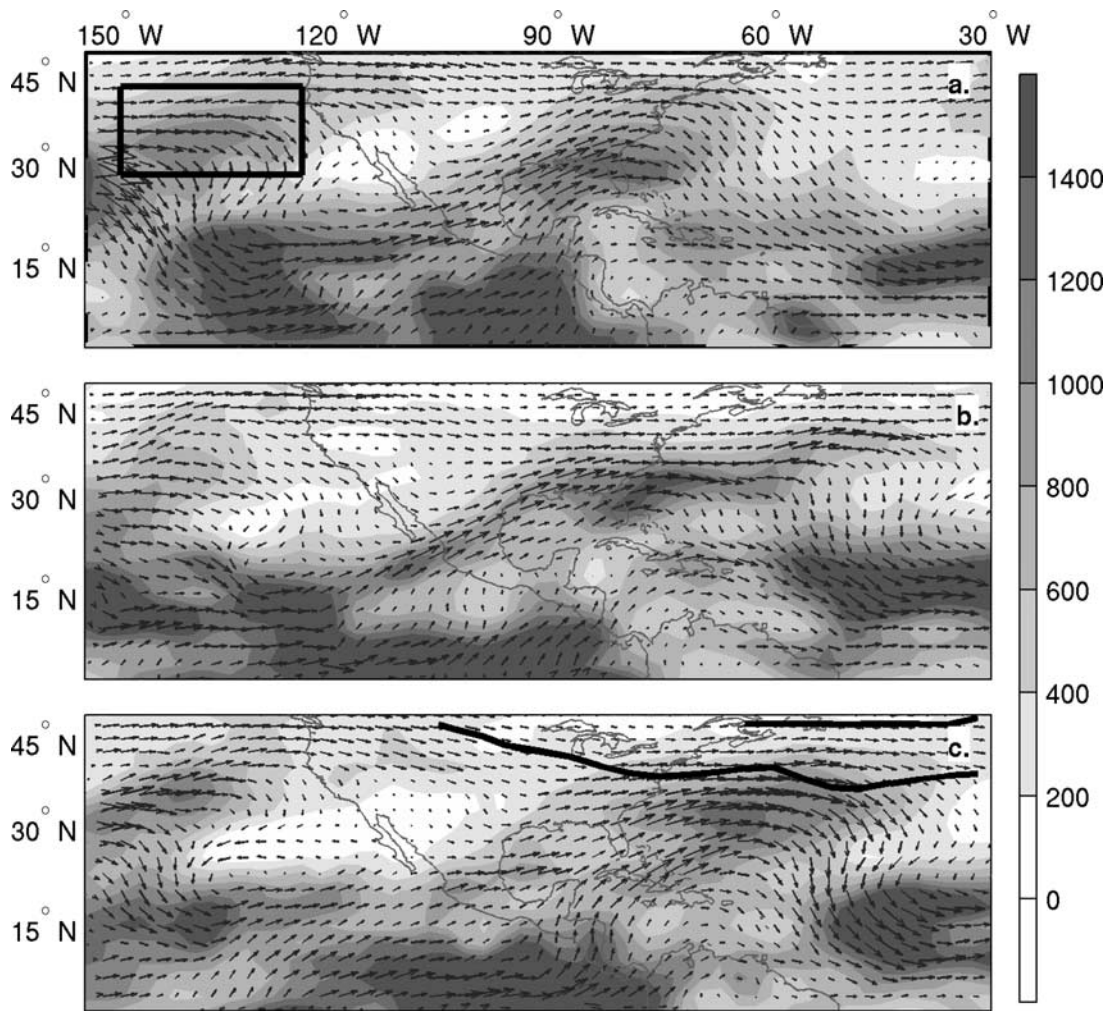


Figure 4. Composite pseudomomentum density (A , shading) and horizontal pseudomomentum flux (arrows) corresponding to observation times (a) 1, (b) 4, and (c) 8 days after an anticyclonic centroid was observed in the east-Pacific box during an upward transition of the NAOI_r (further details in the text). The bold rectangle in Figure 4a bound the east-Pacific box, and the bold curves in Figure 4c bound a portion of the A3 region that is identified by SM08 and referenced in the text. See Animation S1, with a title indicating the lag in days.

posing the horizontal pseudomomentum flux into terms related to advection and propagation, we found that the transport across North America is dominated by advection, which highlights the importance of the spatial scale and configuration of Pacific anticyclonic RWB relative to the subtropical jet.

[13] The composite fields corresponding to four days after breaking (A_4 and horizontal flux, Figure 4b) show a well-defined corridor of pseudomomentum flux from the tropical east Pacific northeastward toward the east coast of the United States, and Animation S1 shows pockets of high pseudomomentum density being advected along this corridor. The break-no-transition-up composite also indicates accumulated pseudomomentum over the tropical east Pacific being advected northeastward, but the break-no-transition-up composite flux field is more zonal over the eastern United States, and the relative absence of flux convergence allows the pseudomomentum to more readily advect eastward over the Atlantic rather than building to the high magnitude shown in Figure 4b. The sign of the flux divergence over the east coast of the United States thus appears to be an

important component that determines whether incoming pseudomomentum from the Pacific will pile up and lead to anticyclonic RWB and the positive polarity of the NAO.

[14] Eight days after the time of Pacific breaking (Figure 4c), the corridor of northeastward horizontal pseudomomentum flux has depleted the pool of concentrated A over the eastern tropical Pacific. The region of high A over the eastern United States has moved out over midlatitudes of the Atlantic, and the Atlantic horizontal pseudomomentum flux on day 8 near 50°W traces anticyclonically-overturning PV. This anticyclonically-overturning PV is closely tied to the development of the positive polarity of the NAO (as discussed in the Introduction). Just poleward of the composite anticyclonic overturning is a portion of the A3 region (bold curves, Figure 4c) in which SM08 showed a correlation between the NAOI and γ_a . To further evidence the temporal progression from east-Pacific breaking to Atlantic A3 breaking and the positive polarity of the NAO, time series showing the composite relative frequency of anticyclonic RWB within the A3 region (denoted $\gamma_a(A3)$) are shown in Figure 3. Considering the phase of the

composite time series, we see that the A3 breaking is positively correlated with the NAO index with essentially zero lag as detailed by SM08, and reaches a local maximum (minimum) several days after the local maximum (minimum) of $\gamma_a(\text{EPac})$.

4. Summary and Discussion

[15] Anticyclonic RWB over a well-defined region of the east Pacific leads to development of the positive polarity of the NAO by initiating a pattern of wave activity flux that forces anticyclonic RWB over the subtropical Atlantic. This inter-basin forcing was evidenced by the finding that upward (downward) transitions of the NAO index are associated with a significantly increased (decreased) relative frequency of anticyclonic RWB over an east-Pacific region centered near 140°W 35°N. Then, composite time series were used to show that Pacific RWB tends to occur several days prior to the Atlantic RWB and the peak of the NAO index. The connection between the Pacific and Atlantic RWB events was shown by analyzing the pseudomomentum flux. Following Pacific RWB, a channel of pseudomomentum flux extends from the Pacific RWB northeastward toward the midlatitudes of eastern North America where pseudomomentum accumulates for several days prior to moving eastward and leading to anticyclonic RWB over the Atlantic.

[16] By directly measuring the relative frequency of RWB by analyzing the occurrence of overturning PV contours, we demonstrated a composite temporal progression from Pacific RWB to Atlantic RWB and the positive polarity of the NAO, and showed that east-Pacific anticyclonic RWB is significantly more likely during upward transitions of the NAO index. We found a fraction of upward transitions of the NAO (13%) for which anticyclonic RWB was absent from the east-Pacific box, and also found 1684 cases of anticyclonic RWB in the east-Pacific

box that occurred while the NAO was moderate but not transitioning up (the cases sampled for the break-to-transition composite). Collectively, the findings here suggest that Pacific anticyclonic RWB is neither necessary nor sufficient for upward transitions of the NAO, but rather increases the probability of anticyclonic RWB over the Atlantic, which is in turn very strongly tied to NAO polarity as shown by SM08. Analysis of the Haynes pseudomomentum flux enabled visualization of this previously undocumented role of the Pacific in the NAO by showing that east-Pacific anticyclonic RWB locally piles up pseudomomentum which is then advected northeastward by the subtropical jet.

[17] **Acknowledgments.** We thank two anonymous reviewers for comments on the manuscript. This work is supported by NOAA Grant NA06OAR4310149 and NSF Grant ATM-0612779.

References

- Benedict, J. J., S. Lee, and S. B. Feldstein (2004), Synoptic view of the North Atlantic Oscillation, *J. Atmos. Sci.*, *61*, 121–144.
- Fleiss, J. L. (1981), *Statistical Methods for Rates and Proportions*, 2nd ed., John Wiley, New York.
- Haynes, P. H. (1988), Forced, dissipative generalizations of finite-amplitude wave-activity conservation relations for zonal and nonzonal basic flows, *J. Atmos. Sci.*, *45*, 2352–2362.
- Magnusdottir, G., and P. H. Haynes (1999), Reflection of planetary waves in three-dimensional tropospheric flows, *J. Atmos. Sci.*, *56*, 652–670.
- McIntyre, M. E., and T. N. Palmer (1983), Breaking planetary waves in the stratosphere, *Nature*, *305*, 593–600.
- Newcombe, R. G. (1998), Interval estimation for the difference between independent proportions: Comparison of eleven methods, *Stat. Medicine*, *17*, 873–890.
- Riviere, G., and I. Orlanski (2007), Characteristics of the Atlantic storm-track eddy activity and its relation with the North Atlantic Oscillation, *J. Atmos. Sci.*, *64*, 241–266.
- Strong, C., and G. Magnusdottir (2008), Tropospheric Rossby wave breaking and the NAO/NAM, *J. Atmos. Sci.*, in press.

G. Magnusdottir and C. Strong, Department of Earth System Science, University of California, Irvine, Irvine, CA 92697, USA. (cstrong@uci.edu)